Annu. Rev. Earth Planet. Sci. 2005. 32:461–91
doi: 10.1146/annurev.earth.33.092203.122459

First published online as a Review in Advance on January 13, 2005

VOLCANIC SEISMOLOGY

Stephen R. McNutt
Alaska Volcano Observatory, Geophysical Institute, University of Alaska, Fairbanks, Alaska 99775; email: steve@giseis.alaska.edu

Key Words volcanic tremor, triggered seismicity, *b*-value anomalies, low-frequency events, very-long-period events

■ **Abstract** Recent developments in volcanic seismology include new techniques to improve earthquake locations that have changed clouds of earthquakes to lines (faults) for high-frequency events and small volumes for low-frequency (LF) events. Spatial mapping of the *b*-value shows regions of normal *b* and high *b* anomalies at depths of 3–4 and 7–10 km. Increases in *b* precede some eruptions. LF events and very-long-period (VLP) events have been recorded at many volcanoes, and models are becoming increasingly sophisticated. Deep long-period (LP) events are fairly common, but may represent several processes. Acoustic sensors have greatly improved the study of volcanic explosions. Volcanic tremor is stronger for fissure eruptions, phreatic eruptions, and higher gas contents. Path and site effects can be extreme at volcanoes. Seismicity at volcanoes is triggered by large earthquakes, although mechanisms are still uncertain. A number of volcanoes have significant deformation with very little seismicity. Tomography has benefited from improved techniques and better instrumental arrays.

INTRODUCTION

Over the past 10 years, volcanic seismology has been a very rich field within geophysics. The quality of data has improved significantly, and many new research methods have evolved or matured. The main focus of this paper is to review recently emerged volcano-specific topics to evaluate significant findings and to place them in perspective by identifying what results are new, as well as what important issues remain to be resolved. The paper has as a secondary focus a discussion of related topics, such as tomography and interferometric synthetic aperture radar (InSAR). For these topics, volcanoes are interesting but not necessarily unique targets. However, the mix of these techniques with volcanic seismology has clearly demonstrated the emerging importance of integrated datasets and multidisciplinary approaches.

This paper is not a comprehensive review of the entire field, which would be impossible in a paper of this length, nor is it the intended purpose. Rather, this paper is intended to be a balanced overview of the current status of the field of

volcanic seismology. In several instances I have chosen to present new material in figures to illustrate developing ideas. This has the advantage of introducing new data to the literature rather than merely reproducing existing figures. The emphasis given to selected topics, and any errors or omissions in content, are entirely my own.

Terminology

Terminology remains a problem for volcanic seismology. Although a consensus on terminology is desirable, one is not likely to emerge any time soon. Here a few observations and recommendations are made, chiefly to clarify how terminology is used in this paper and to discuss how terminology has occasionally caused problems that have impeded research. The four basic types of events, high-frequency (HF) earthquakes, low-frequency (LF) earthquakes, explosions, and volcanic tremor, have been described in the literature repeatedly (e.g., Minakami 1974, Lahr et al. 1994, McNutt 1996, Zobin 2003). Of these, the LF events are the troublemakers. Attempts to classify them by frequency content may work at individual volcanoes, but there is overlap with "normal" earthquakes (Figure 1), and it is not clear that similar events at two different volcanoes are necessarily caused by the same physical mechanisms. Spectral ratios have been used as a quantitative method to distinguish event types with illuminating results (Neuberg et al. 2000) and demonstrate that instead of two types of events with different "dominant" frequencies, there is in fact a complete spectrum of events with variable relative frequencies (Figure 2). Another approach was taken by Falsaperla et al. (1996), who used multilayered neural network algorithms to classify objectively the seismic events at Stromboli. Many workers use the term long-period (LP) events. This is an unfortunate choice because it is in conflict with traditional use of "long period" in seismology to represent the instrumentation as well as that part of the earthquake energy at periods longer than the Earth noise peak at approximately 10 s. There are local events at volcanoes with such long periods, but they now need to be called very-long-period (VLP) events. Both of these terms are descriptive and eventually may be replaced by genetic terms as understanding improves.

Figure 1 Plot of seismic moment versus corner frequency for individual earthquakes from different places (*key upper right*) with frequency and moment ranges for volcanic low-frequency events superimposed (*various shaded patterns*). The individual points represent normal tectonic earthquakes. Frequencies of LF events (whose spectra are generally more peaked) overlap in approximately half of the cases, demonstrating that frequency alone is not a clear diagnostic. Magnitudes were converted to moments using the relation in Archuleta et al. (1982, p. 4603). Earthquake data are from Haar et al. (1986). Volcano data used to make the plot are given in table 2 in McNutt (1989).

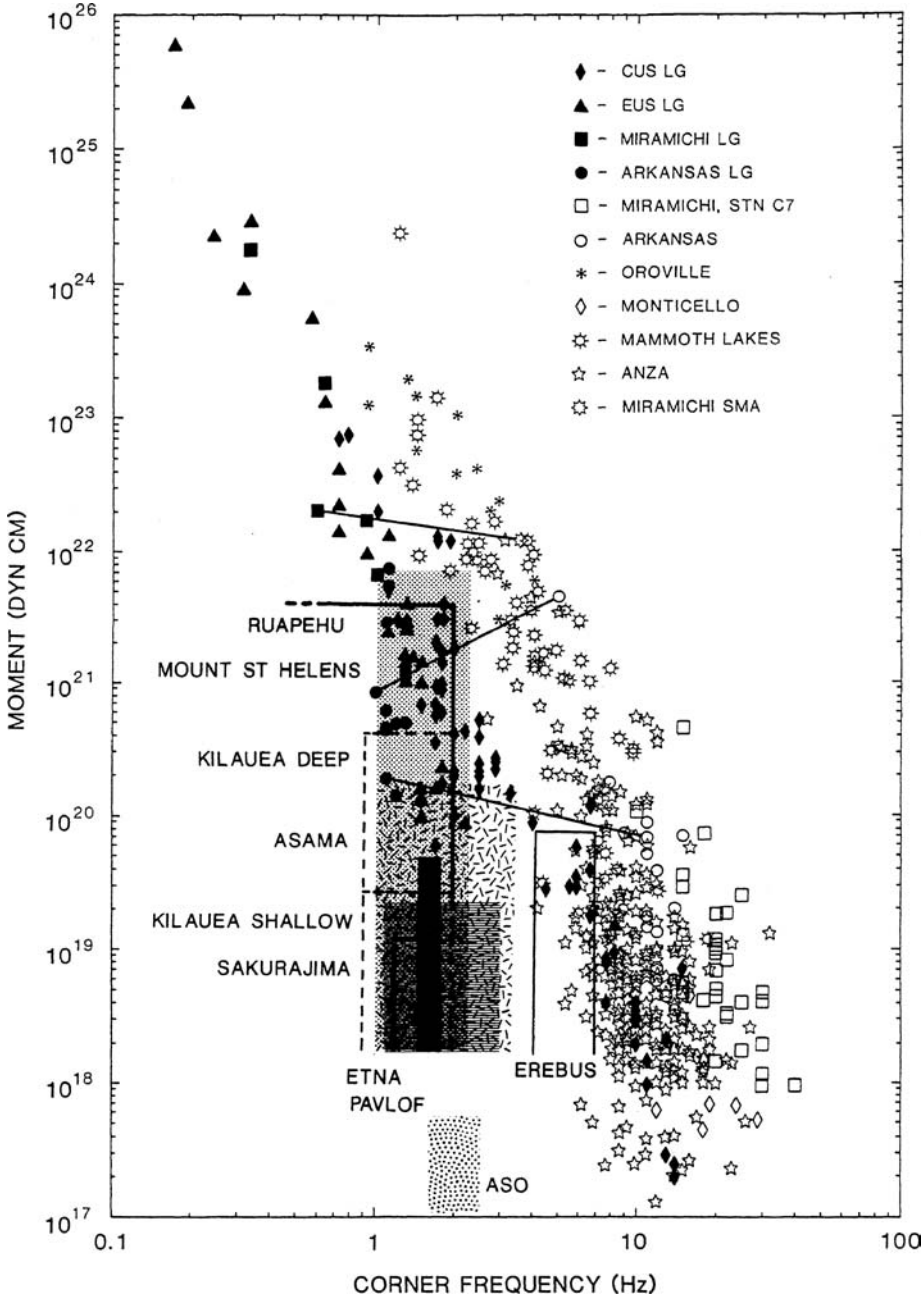

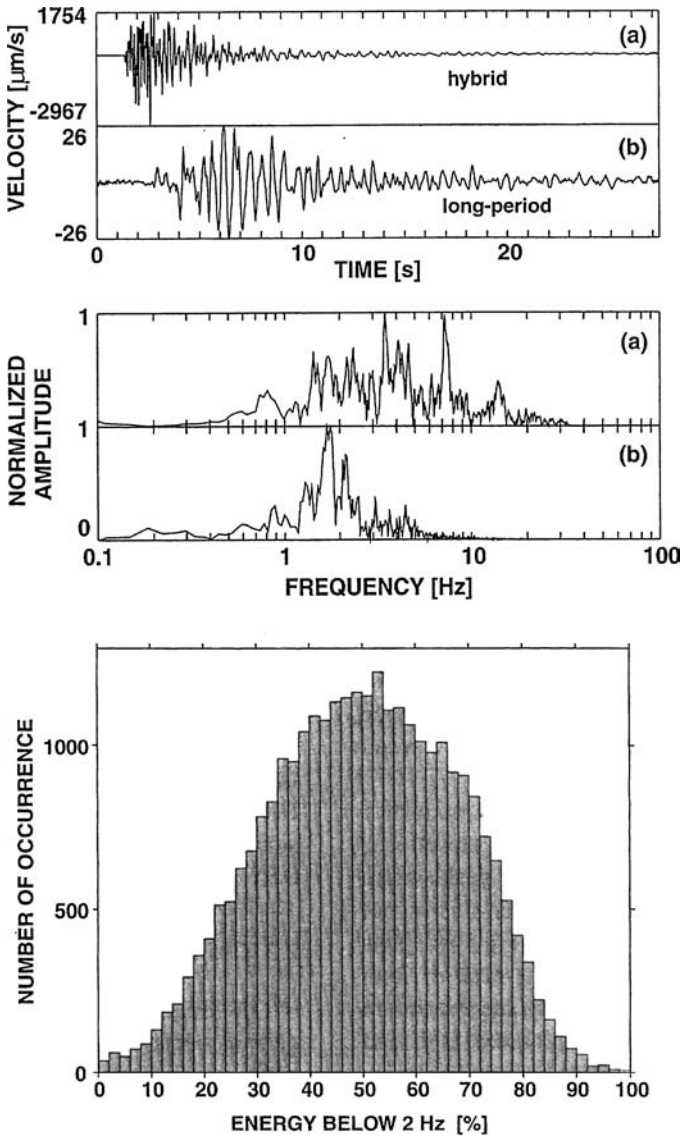

Figure 2 Top: Typical seismograms and spectra for (*a*) a hybrid earthquake and (*b*) a low-frequency or long-period event. Data from Montserrat volcano station MBGA, vertical component. Bottom: Histogram of low-frequency events according to their fraction of energy below 2 Hz. Data based on analyses of velocity seismograms from station MBWH. The distribution demonstrates a continuum between low-frequency and hybrid events. For distinct event types one would expect a bimodal distribution (after Neuberg et al. 2000).

HIGH-FREQUENCY EVENTS

High-frequency events [also called volcano-tectonic (VT) events] are relatively understudied considering the pervasiveness of earthquake swarms at volcanoes. The process that causes the HF events, shear fracture, is well understood and may partly explain this. HF events are useful at volcanoes to determine stress orientations via study of focal mechanisms and stress tensor inversion (e.g., Moran 2003, Sanchez et al. 2004, Waite & Smith 2004). Unusual mechanisms, including many nondouble couple events, have been determined for earthquakes with otherwise normal frequency content in the Hengill region of Iceland (Julian et al. 1997). Recently, a number of studies have examined triggering of seismicity by distant large earthquakes (e.g., Gomberg et al. 2001, Power et al. 2001, Hill et al. 2002, Toda et al. 2002, Brodsky et al. 2003). The triggered events are predominantly HF events, so these studies help show that stress conditions at volcanoes are near critical, so that changes induced by passing waves can modify temporal patterns of occurrence. Triggering appears to be well established even though the underlying mechanisms are not well understood.

Perhaps the greatest progress in studying HF events has been the implementation of a suite of techniques used to improve locations. The double difference method (Waldhauser & Ellsworth 2000) exploits the residuals between observed and calculated travel time differences for pairs of earthquakes at common stations to give very precise relative relocations. This technique is well suited to areas that have high density of stations and well-distributed seismicity. For example, Prejean et al. (2002) applied the technique to Long Valley caldera and relocated 45,000+ earthquakes. They were able to define many faults that were not discernable in standard locations (Figure 3) and then study the distribution of stresses on the individual faults. Other techniques relying on waveform alignment, such as an automatic method based on (*a*) cross-spectral phase estimation, (*b*) cross coherency-based filtering, and (*c*) stacking, work well in areas with fewer stations but many earthquakes that share similar waveforms (Rowe et al. 2002). These techniques have been applied successfully to Redoubt (C. Rowe, written communication) and Pinatubo (Battaglia et al. 2004) volcanoes. In all the areas mentioned, diffuse clouds of earthquakes have been shown to originate from a small number of well-defined sources, which can be interpreted as faults or other structures.

The problems of earthquake location and of velocity structure determination are interdependent. Thus, recent studies have performed joint inversions for locations and velocity structure (e.g., Chiarabba et al. 2000, Zhang & Thurber 2003). In addition to the intrinsic merit of better locations, the new locations and velocity models can then provide revised takeoff angles so that focal mechanisms may be improved. It is clear that accurate velocity models and earthquake locations are fundamental to seismology and affect the interpretation of all derivative information (see also Tomography, below).

Causes of HF events, that is, the sources of the stresses, have been attributed to regional tectonic forces, gravitational loading, pore pressure effects and

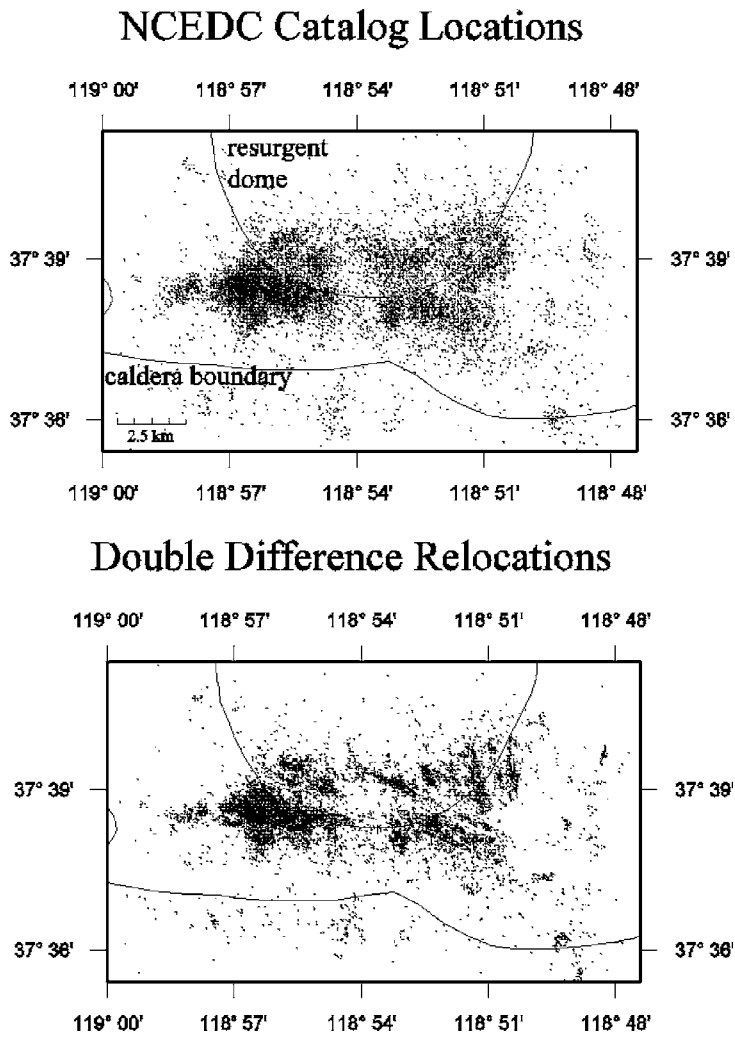

Figure 3 Long Valley caldera seismicity for the period July 1997 to January 1998. Upper panel shows initial Northern California Earthquake Data Center catalog locations. Lower panel shows double-difference relocations (Waldhauser & Ellsworth 2000) using P-phase catalog arrival times (after Prejean et al. 2002).

hydrofracturing, thermal and volumetric forces associated with magma intrusion, withdrawal, cooling, or some combination of any or all of these. Moran (2003) discusses these possible mechanisms with respect to HF events at volcanoes in Katmai National Park, Alaska. Ocean bottom seismometer (OBS) deployments on the seafloor have allowed characterization of shallow HF seismicity associated with high-temperature vent fields in the East Pacific Rise (Sohn et al. 1999). Kilburn (2003) examined extension of faults by time-dependent

reactivation of cracks at different scales and was able to reproduce rates of earthquakes theoretically that closely resemble observed cases of volcanic earthquake swarms.

Generic Swarm Model

Independent of event locations, temporal patterns of earthquake occurrence may be studied for clues to help identify magmatic processes. For example, a generic volcanic earthquake swarm model was published a few years ago (McNutt 1996) chiefly to provide a conceptual framework for discussion. It is obvious that no single model will represent every possible case; the generic model provides a sufficiently high number of elements so that the key underlying processes can be identified. The basic elements of the models are HF swarm onset, peak rate, relative quiescence, occurrence of LF events and tremor, eruption, and posteruption seismicity. One new result, published here for the first time, is that swarms preceding eruptions are shown to have two dominant processes acting: one before the peak rate occurs and one after (Figure 4). The durations of the postpeak portions of the swarms are proportional to the peak rates (Wilson & McNutt 1998); this is similar to

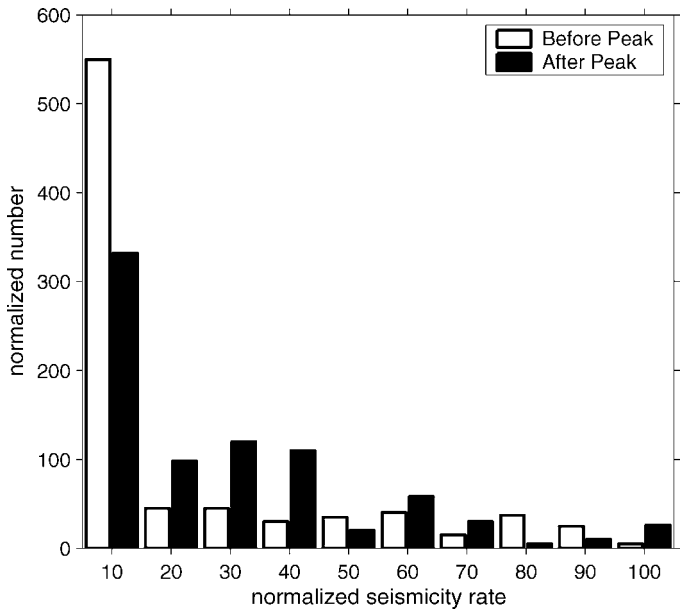

Figure 4 Histograms showing the normalized number of events per bin for 20 volcanic earthquake swarms. For each swarm, the peak rate (e.g., number of events per day) was assigned a value of 100%; the rates for other days were then measured and tabulated separately for 10% bins before and after the peak. The two distributions are significantly different, suggesting that different processes govern the distributions (after Wilson & McNutt 1998).

the behavior of aftershock sequences and suggests that diffusion is a controlling process. The portions of the swarms prior to the peaks behave differently, however. These may represent the invasion of hot fluids and the reopening of cracks prior to intrusion. More study is required to identify these processes unambiguously.

The sequence of events of the generic swarm has occurred over various earthquake magnitudes, eruption sizes, and durations, including 2 months prior to a Volcanic Explosivity Index (VEI) = 5 dacite eruption of Mount St. Helens in 1980 (Malone et al. 1981), 10 months before a VEI = 3 andesite eruption of Mount Spurr in 1992 (Power et al. 1995), 3 weeks preceding a submarine basalt eruption (equivalent VEI = 2) at Ito-oki in 1989 (Ukawa 1993), and 18 days before a VEI = 1 phreatic eruption at Colima (Jimenez et al. 1995). Because the individual eruptions vary so widely, the sequence of seismic events most likely represents a common overriding process, such as ascent of magma and volatiles. The timescales are quite different, depending on the ascent rate, and bear no obvious relation to magma composition or volume. For the cases cited, the stress conditions prior to the swarms are not well known. Such information will eventually be needed to determine the significance of changes and to determine mechanisms.

b-Value Spatial Mapping

The frequency-magnitude relation is one of the most widely studied topics in seismology (Bath 1981). It is generally known to seismologists as the *b*-value because *b* is the slope of the equation written as $\log_{10}N = a - bM$ (Richter 1958), where N is the cumulative number of earthquakes, M is the magnitude, and *a* and *b* are constants. For tectonic areas, the *b*-value is nearly always close to 1.0 (Frolich & Davis 1993); however, in volcanic areas, very high values have been observed. Wiemer & Benoit (1996) first used a dense spatial grid to study *b*-values at four subduction zones; later, studies were extended to volcanoes. At present, 13 volcanoes have been studied using this technique (Table 1). Such studies require a well-distributed group of earthquakes; if the events all occur at one point then no meaningful spatial mapping can be done. All volcanoes studied to date have shown high spatial variability of *b*, with regions of normal *b* (1.0) adjacent to regions with anomalously high *b* (up to 3.0). In general, *b* is high at depths of 7–0 km where the earthquakes are adjacent to inferred magma bodies identified by other techniques. However, approximately half of the studied volcanoes also show significant high *b* anomalies at depths of 3–4 km (Table 1). This is the approximate depth at which magma with 4 wt% gas starts to exsolve the gas, and further, is near the depth at which open cracks may exist in the host rock. The data sets used for these analyses show that the *b*-value anomalies are long-lived (years to decades) features. This is somewhat in contrast with previous studies of *b* as a function of time (e.g., Main 1981, Gresta & Patane 1983), or rather, the documented spatial variation has created an ambiguity in interpreting whether *b* varies as a function of space, time, or both.

A new result published here for the first time is the elucidation of a common temporal pattern of *b* for earthquake swarms associated with eruptions and intrusions (Figure 5). The *b* changes from a normal background value to a short-lived

TABLE 1 b-value anomalies and depths at volcanoes

Volcano	b	Depth (km)	References
Coso	1.7	0.8–3	M. Wyss, written communication
Mount Spurr	1.7	3–4 8–10	Wiemer & McNutt 1997
Mount St. Helens	1.8	3–4 7–8	Wiemer & McNutt 1997
Redoubt	1.7	3–4 6–8	S. Wiemer, written communication
Mammoth Mtn.	1.6	3–4 7–9	Wiemer et al. 1998
Long Valley (resurgent dome)	1.8	3–11	Wiemer et al. 1998
Ito-oki	1.5	7–15	Wyss et al. 1997
Martin/Mageik	1.8	3–7	Jolly & McNutt 1999
Katmai	1.6	6–8	Jolly & McNutt 1999
Montserrat	1.6	1–5	Power et al. 1998
Kilauea	1.9	4–7 (E Rift) 20 (S of crater) 1 (below crater)	Wyss et al. 1998
Etna	1.8	13 (2 km E of summit)	Murru et al. 1999
Oshima	1.5	4 (4 km NW of summit)	M. Wyss, written communication
Pinatubo	1.7	0–4 (NE of vent) 8 (SE of vent)	Sanchez et al. 2004

high, then decreases, then increases again to a secondary (generally lower) high with a longer time constant, eventually returning to a low background level. Based on knowledge of *b* from lab and field studies, these observations suggest that the short-lived high *b* is probably a result of high thermal gradients (Warren & Latham 1970) that dissipate quickly. The heat may be carried by gasses, liquid water, or magma. The longer-lived secondary high *b* is consistent with an increase in pore pressure, similar to observations at Rangely, Colorado, in association with fluid injection in deep wells (Wyss 1973). This suggests that diffusion is a main controlling factor. A comparison of methods used to compute *b* at Etna is given by Centamore et al. (1999).

Note that *b*-value anomalies are features of the earthquakes themselves and the space they occupy. This is in contrast to tomography studies in which the rays from earthquakes pass through the region of interest, but the earthquakes themselves are not required to be within it (see also section below on tomography). The

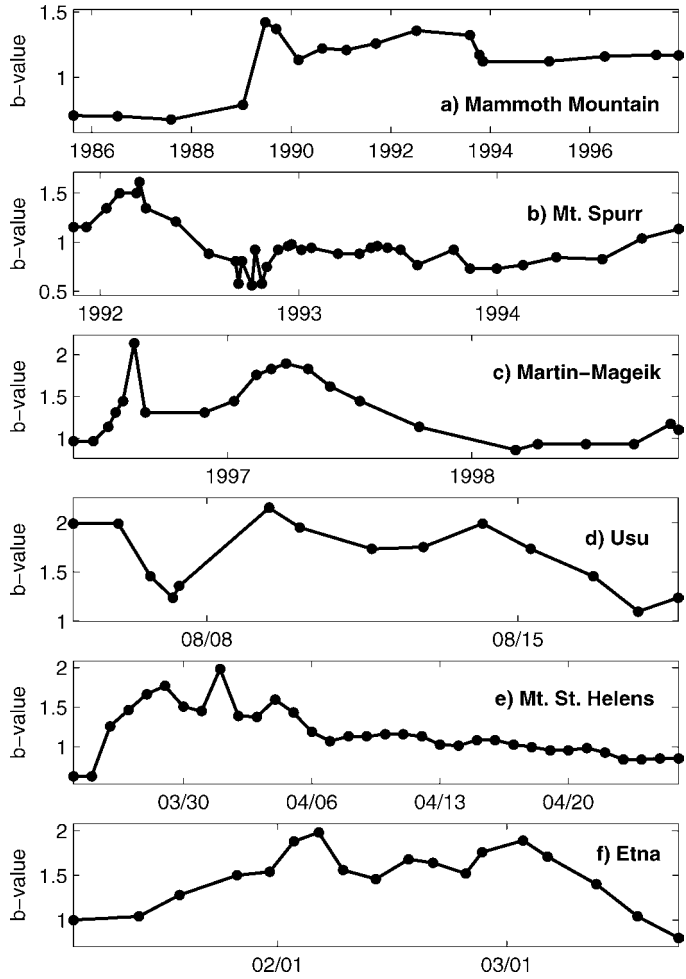

Figure 5 *b*-value versus time for six volcanic earthquake swarms: (*a*) Mammoth Mountain, California, 1989 (Wiemer et al. 1998); (*b*) Mount Spurr, Alaska, 1992 (S. Wiemer, written communication); (*c*) Mounts Martin and Mageik, Katmai region, Alaska, 1996 (Jolly & McNutt 1999); (*d*) Usu Volcano, Japan, 1977 (Suzuki & Kasahara 1979); (*e*) Mount St. Helens, Washington, 1980 (R. Crosson, written communication; S. McNutt, unpublished data); and (*f*) Mt. Etna, 1983 (Gresta & Patane 1983). Each case shows a short-term high *b* near the swarm onset, followed by a decline then by a sustained high *b*, and followed by an eventual return to near background levels. See text for further explanation.

b-value techniques, although powerful, are limited to those regions that produce earthquakes in sufficiently high numbers to perform the analyses.

LOW-FREQUENCY EVENTS

Low-frequency (LF) events (also called long-period or LP events) continue to be treated as the holy grail of volcanic seismology. Whereas HF events are caused by a known process (shear fracture), LF events are thought to be caused by fluid processes that are still not well understood. Hence, there are several alternative mechanisms and models (e.g., Julian 1994, Chouet 1996, Nakano et al. 1998, Neuberg & O'Gorman 2002, Fujita & Ida 2003) and some disagreement about the relative contributions of factors such as coupling at walls, geometry of conduits, and origin of mechanical energy. For these events there is also a fundamental ambiguity about defining the source, whether this is the source of mechanical energy alone or the ensemble of mechanical source and fluid-filled conduit that radiates energy. The latter is closer to what seismologists call the source for tectonic earthquake studies (the entire fault surface), whereas the former is perhaps of greater concern to volcanologists who seek an understanding of the driving forces. For example, if the LF events are caused by gas pressurization in conduits, then understanding the occurrence rate could enable estimates of the amount of magma and gas flux (e.g., Neuberg 2000). Using seismology to quantify magma movement and evolution is a long-term goal of the science.

Despite the ambiguity regarding the source, many authors have studied these events, focusing on particular features such as spectral content, rates, or relation to eruptions. Several new studies have taken a more complete approach by examining wavefield effects such as varying magma properties with depth and modes of seismic energy leaking from various positions along the conduit (e.g., Neuberg & O'Gorman 2002). Nishimura & Chouet (2003) used finite difference numerical simulations to model dynamics of magma flow simultaneously in a conduit and reservoir. The models agree qualitatively with observed radiation of seismic energy (both LP and VLP events) and crustal deformation in the vicinity of the volcano. In particular, the models help explain some of the processes and sequence of events that occur when a deep (2 km) pressure fluctuation triggers an explosive eruption at the surface, as has occurred repeatedly at Sakurajima (Iguchi 1995). These studies are welcome because the additional processes described and modeled have fairly strong effects on the resulting seismograms and are now beginning to be understood quantitatively.

LP events at Kilauea volcano have been relocated using a two-stage procedure by Battaglia et al. (2003). First, amplitudes as a function of hypocentral distance (corrected for site effects) are computed, based on amplitude decay of body waves. This is followed by precise relative relocation of events based on waveform similarity. At Kilauea, clouds of events 4–8 km in diameter have been relocated to small volumes 0.5–1 km in diameter (Figure 6). Note that these are volumes rather than lines, hence they indicate volume sources rather than planar faults.

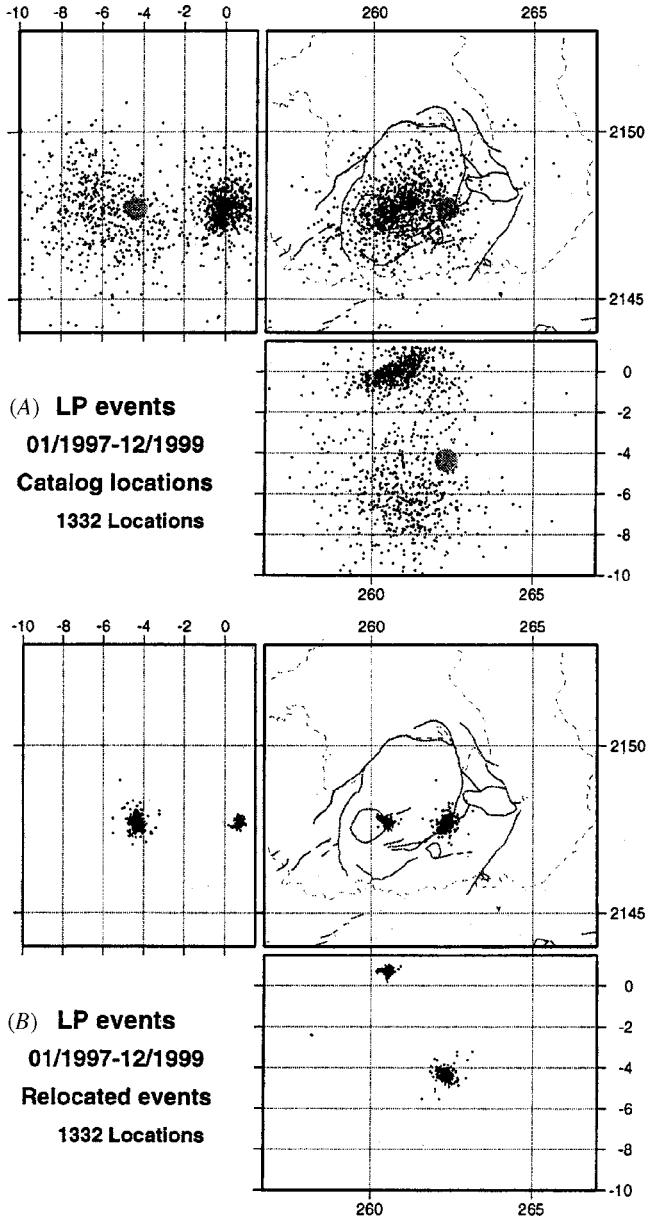

Figure 6 Comparison between (*A*) original catalog locations and (*B*) relocated events for the same group of long-period events at Kilauea volcano. Map views and north-south and east-west cross sections are shown; depths are in km. The position of the prominent cluster of deep events is added to the left plot for comparison; its absolute location was determined from amplitude locations (after Battaglia et al. 2003).

Finally, the possibility remains that some events that have been called LF or LP events are really normal earthquakes for which the rupture occurs at a slower timescale. The scatter in "normal" earthquakes shown in Figure 1 and the overlap between normal and LF events, also shown in Figure 1, certainly suggest that this is the case for some events. True LF events, however, lack S phases and have longer codas than normal events. Applying all these diagnostics strictly can help improve event discrimination.

Deep Long-Period Events

Deep LP events (20–40 km, near the base of the crust) have been the object of intensive study for several reasons. First is their ubiquity; whereas previously only a few case studies existed, recent studies have shown that they occur beneath one third (9 out of 27) of monitored Alaskan volcanoes (Table 2; Power et al. 2004), although the rates, depths, and sizes vary considerably. Additional cases worldwide are given by White (1996) and McNutt (1994b). Second is the discovery of deep aseismic slip events at subduction zones based on GPS data (Dragert et al. 2001); most of these are accompanied by swarms of deep LP events. In Japan, the occurrence of deep LP events throughout the islands was documented by Obara (2002), following the installation of a dense national network of broadband seismometers. These small events were identified and located by cross correlation of the waveforms rather than by conventional picking of arrival times. Further, these events are rich in S waves, whereas volcanic LF or LP events typically lack an S phase. The deep slab events are thought to be associated with high fluid pressures in the mantle wedge; because dewatering of the slab is a likely candidate process, the fluid is likely to be water. In volcanic cases, however, anomalously

TABLE 2 Deep long-period events at volcanoes in Alaska[a]

Volcano	Depth (km)	f (Hz)	No. events	Period
Spurr	10–40	2–2.6	93	1989–2002
Redoubt	31	1.8–2.8	6	1989–2002
Iliamna	24–30	2–4	3	1989–2002
Katmai cluster	33	1.2	10	1995–2002
Aniakchak	23	1.6	10	1997–2002
Pavlof	18	3.3	3	1996–2002
Shishaldin	27–52	2–4	13	1997–2002
Makushin	22–32	2–4	6[b]	1996–2002
Great Sitkin	25–33	2–4	2	1999–2002

[a]Data from Power et al. 2004.

[b]Includes additional data from AVO unpublished data (J. Sanchez, written communication).

high CO_2 output at the surface has been seen some time after the onset of deep LP events, such as at Mammoth Mountain, California (Hill 1996), and correlates closely with a Vp/Vs low anomaly (Julian et al. 1998). This suggests that CO_2 is an important fluid involved in the source processes of deep volcanic LP events. Regrettably there are few additional supporting data to provide clues about source mechanisms. It is possible that some events that have been identified as deep LP events are normal earthquakes whose high frequencies have been filtered out; the travel paths are longer because of the depths, and further, the deep crust is partly plastic and may be fluid rich. Both of these factors may increase attenuation.

VOLCANIC EXPLOSIONS

Volcanic explosions have been well studied in recent years. Calibrated infrasonic microphones or infrasonic pressure sensors have been installed in more than a dozen volcanoes to complement seismic networks (Johnson 2000, Caplan-Auerbach & McNutt 2003), and these have permitted the recording of tens to thousands of explosions. Key issues include the depth, the coupling of energy between the ground and air, and the seismic or acoustic efficiency, which may be defined as the amount of radiated seismic or acoustic energy versus kinetic or thermal energy. Nishimura (1998) showed that the seismic magnitude for the largest explosion event at each volcano is proportional to the cross-sectional area of the vent. Explosion depths may be as shallow as a few hundred meters; however, studies at Sakurajima have shown a signal originating at a depth of 2 km that immediately precedes and is likely coupled to the part of the process that produces the explosion at the surface (Iguchi 1995, Uhira & Takeo 1994). The nature of the coupling is an open question. There may be fluid transfer involved, or the passage of a wave may link two distinct physical processes (e.g., Nishimura & Chouet 2003). For example, a small earthquake at depth might produce a P wave that travels upward and triggers disruption of a gas bubble near the surface.

Acoustic waves in the atmosphere are not affected as much by propagation effects as are seismic waves in the ground (Garces et al. 1998, Garces 2000). Thus acoustic data give a more direct view of some explosive and eruptive processes. Aster et al. (2004) used combined seismic, acoustic, GPS, radiometer, and video data to study explosions at Erebus Volcano, Antarctica. They found strombolian explosions that produced VLP signals, simple acoustic pulses, more complicated seismic signals, irradiance pulses, and video imagery. All these data were transmitted via the internet, thus demonstrating that integrated digital data can be obtained despite the hostile, remote location.

VOLCANIC TREMOR

Volcanic tremor remains the most distinctive volcanic seismic signal recorded at volcanoes. Tremor is generally denoted by its narrow frequency range or sharply peaked spectra and its long duration compared with earthquakes. Whether tremor

is truly continuous depends partly on the source; it is well known that impulsive sources such as man-made explosions can produce long seismograms because different waves are produced that travel at different speeds and because of multipathing, including reflections and refractions. Tremor attributes also reflect features of the recording systems, all of which have thresholds. Many investigators lump tremor together with LF events because of shared spectral characteristics; however, the driving forces are likely different. Benoit et al. (2003) showed that tremor durations scale with an exponential law rather than a power law, in sharp contrast to well-established scaling laws for earthquakes (see *b*-Value Spatial Mapping, above). This implies that there is a scale bound for tremor, such as a fixed conduit length or a constant pressure. In contrast, earthquakes are generally unbounded; an earthquake of any size can occur on a very long fault and/or a fault can grow to accommodate a larger earthquake.

A very interesting and beautiful feature of tremor is referred to as gliding, in which the frequencies of evenly spaced spectral peaks vary systematically with time. The same peaks, gliding the same way, have been observed simultaneously on seismic and acoustic sensors at Arenal Volcano (Figure 7, see color insert), demonstrating that the source is coupled across the air-magma interface, which acts like a drumhead (Garces et al.1998). Changing source lengths, bubble concentrations, or more likely pressures, all of which change acoustic velocities, have been modeled as the likely causes of the gliding (Neuberg & O'Gorman 2002). Neuberg (2000) also suggests that changing the trigger frequency, as opposed to material properties, can produce similar spectral gliding. Hellweg (2000) studied additional cases of gliding and introduced several novel mechanisms, including vortex shedding, turbulent slug flow, and periodic degassing, such as that which occurs in a soda bottle.

A number of studies have shown evidence of changing apparent source depths of tremor. These suggest that the source is extended; that is, a line source rather than a point source. For example, Benoit & McNutt (1997) used S wave polarization data to infer changing source depth at Arenal Volcano over a span of approximately 10 s. Models by Neuberg & O'Gorman (2002) as well as others explicitly involve energy emanating from an extended source.

Tremor remains very useful for estimating the VEI of eruptions while they are in progress. This is done by measuring tremor on a normalized amplitude scale known as reduced displacement or D_R (Aki & Koyanagi 1981). An original relation between D_R and VEI relied mostly on central vent eruptions from stratovolcanoes (McNutt 1994a). New data have been added here with an emphasis on different types of eruptions. These new data reveal that tremor is systematically stronger for fissure eruptions, phreatic eruptions, and eruptions with higher gas content (three data pairs of gas-rich and gas-poor eruptions from the same vents). Figure 8 shows the new data superimposed on the old data using letters F (fissure), P (phreatic), H (high gas), and L (low gas) to illustrate the points above. The stronger tremor from fissure eruptions is likely a geometric effect because of the greater surface area and ease of opening a crack as opposed to enlarging a cylindrical conduit. Stronger tremor for phreatic eruptions suggests an efficient

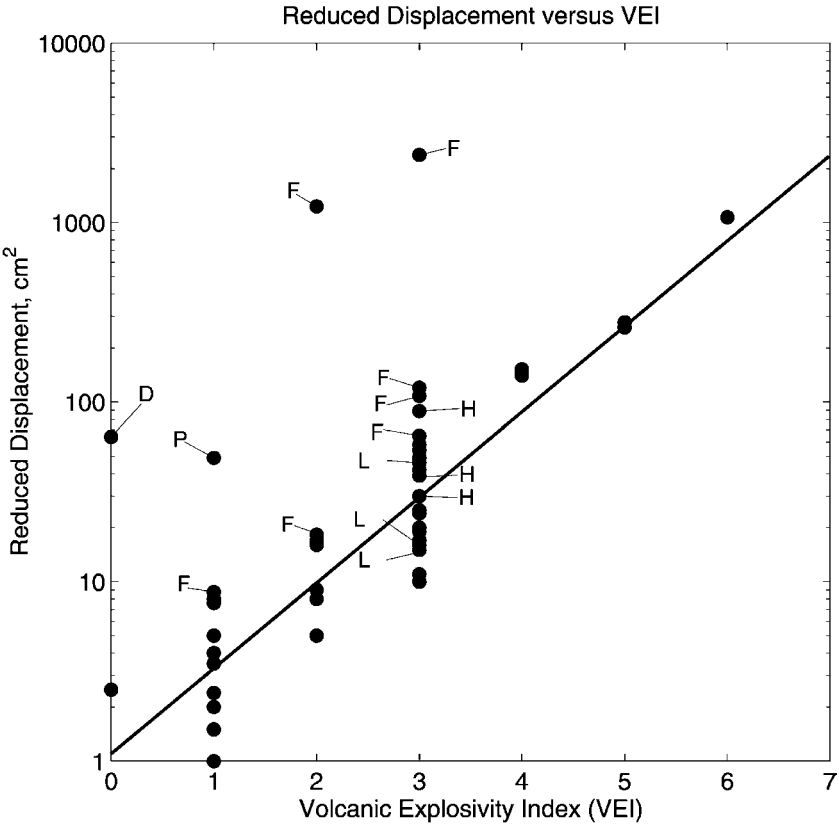

Figure 8 Reduced displacement, a normalized measure of amplitude, versus the Volcanic Explosivity Index for 50 eruptions at 31 volcanoes. The regression line is from McNutt (1994a), based on a smaller data set, and is shown for comparison. Fissure eruptions are labeled F, a phreatic eruption is labeled P, deep (40 km) tremor from Kilauea is labeled D (no eruption for this one), and three pairs of values from VEI = 3 eruptions with high and low gas content are labeled H and L, respectively. See text for further explanation.

conversion of thermal to mechanical energy as groundwater is cooked. Gas content is a bit more problematic to explain; higher gas content in magma provides more driving force but also poorer coupling between the magma and conduit walls because of higher impedance contrast. Nevertheless, all three cases in Figure 8 show the same polarity and magnitude of a factor of 2 stronger tremor for higher gas content. Advance knowledge of vent geometry and eruption type can improve estimates of likely size (VEI) of eruptions by allowing calculations based on conditional probabilities for which the data set can be divided.

PATH AND SITE EFFECTS

Although source studies retain the glamour, path and site effects at volcanoes are sufficiently extreme that they warrant additional attention. Many studies try to determine the "dominant" effects. This approach works; however, an alternative would be to determine the relative contributions of source, path, and site effects in interpreting seismograms. Figure 9*B* shows three-component seismograms from three small earthquakes near Mammoth Mountain, California (previously unpublished). Both the P and S waves are distinct for the events that occur at a depth of approximately 4 km and epicentral distance of 3 km (Figure 9*A*). The station MMB is located on an old dome and is essentially a bedrock site. Figure 9*C* shows the same events at an adjacent site that is approximately 4 km epicentral distance. The seismograms look completely different. Whereas the earthquakes appear to be ordinary HF events at station MMB (Figure 9*B*), on station MMF (Figure 9*C*) the events look like a single LF event with extended coda. The third event can be discerned barely, but the small second one cannot even be identified. Station MMF is a soft sediment site. The network geometry was designed to record optimally for focal mechanism studies (B. Julian, personal communication). This example clearly demonstrates the high impact of path and site effects on the resulting waveforms.

Path effects including P wave anisotropy and inferred crack density, stress distribution, and permeability were determined for the Coso geothermal field, California, by Lees & Wu (1999). Site effects have been studied using a linear array at Arenal Volcano (Mora et al. 2001). Over short distances of 150 to 500 m, the horizontal/vertical spectral ratios varied considerably, suggesting that shallow sediment (tephra) layers strongly influence the seismograms. The amplification is generally strong around 2 Hz, which is a typical frequency for tremor (see also Figure 7). One station has a strong peak at 3.5 Hz. Such studies are steps in the right direction in terms of coming to grips with the complicated structures of volcanoes and the effects these structures have on resulting seismograms.

VERY-LONG-PERIOD EVENTS

The widespread use of broadband seismometers in the past decade has produced a suite of interesting new data on VLP events. These signals have periods ranging from 3 to 100 s or longer (Table 3). There are several ways to view these signals: Either they are a new phenomena of which we were previously unaware, or they are a scaled-up version of existing processes, or they are waves from known processes that we simply could not see before. Perhaps the most interesting feature of the observations is the fact that quite small source regions have been shown to create VLP signals. This is a departure from linearity (for linear processes, large structures would be needed to produce long periods) and suggests that the broadband

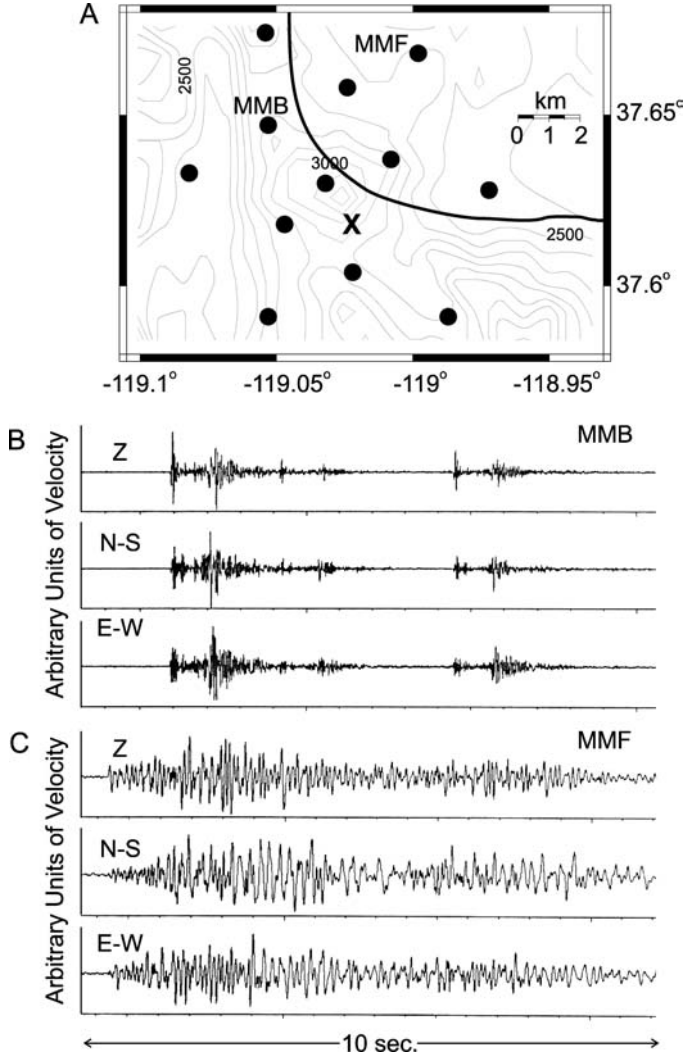

Figure 9 (*A*) Map of temporary seismic stations (*dots*) deployed near Mammoth Mountain, California, in 1989 (after Julian et al. 1998). The edge of Long Valley caldera is the heavy curved line. The approximate location of the earthquakes is shown as a cross. (*B*) Vertical, north-south, and east-west seismograms from station MMB. 10 seconds of data are shown. Clear P and S waves can be seen for three small earthquakes beginning roughly 1.5, 3, and 7 seconds into the record. (*C*) The same events for vertical, north-south, and east-west seismograms from station MMF. Note that the seismograms look like a single low-frequency event. The third event can be identified with close scrutiny, but the small second one cannot be seen. This is a clear example of site effects.

TABLE 3 Very-long-period event characteristics

Volcano	Period(s)	Features	References
Kilauea	10	Associated with SP swarm	Ohminato et al. 1998
Stromboli	3–6	Associated with explosions	Neuberg et al. 1994
Aso	15	Always emitted	Kawakatsu et al. 2000
	3–15	Hydrothermal; 1.8 km deep	Kaneshima et al. 1996 Yamamoto et al. 1999
	100	Precedes eruptions	Kawakatsu et al. 2000
Sakurajima	2.5–5	Many various waveforms	Kawakatsu et al. 1992
Satsuma-Iwojima	5	Shallow, periodic 46–50 m	Ohminato & Ereditato 1997
Mount	7–20	Associated with explosions	Rowe et al. 1998, 2000
Erebus			
Unzen		Pyroclastic flows	Uhira et al. 1994
Iwate	10	Associated with swarms	Nishimura et al. 2000
Miyake	50	Depression of crater	Kumagai et al. 2001
Mount St. Helens	150	Onset of May 18, 1980 eruption	Kanamori & Given 1982
Pinatubo	228–270	Accompanied climactic eruption	Kanamori & Mori 1992
Hachijo Is.	10	Modeled as basalt-magma-filled crack	Kumagai et al. 2003

data are revealing a new class of processes. For example Kawakatsu et al. (1994), Kaneshima et al. (1996), and Yamamoto et al. (1999) reported and modeled VLP signals emanating from hydrothermal processes at Aso Volcano. A small (1 km) source region produced waves with periods of 10–15 s, corresponding to draining of a water-saturated crack-like conduit at shallow depths. At Stromboli, VLP signals precede small explosive eruptions by several seconds and have been modeled as upward movement of gas slugs prior to eruption (Neuberg et al. 1994). The explosion events themselves produce short-period signals. VLP events at Kilauea have been modeled as pulses of magma flow through sill-like cracks (Ohminato et al. 1998). Each pulse corresponds to modeled flow of 700 m^3 of magma. At Iwate Volcano, a 4-km-long extended source with simultaneous expansion and dilatation was modeled by Nishimura et al. (2000). Study of VLP events has introduced a whole series of interesting new models of magmatic and hydrothermal processes. The variety of signals recorded suggests that there must be several different processes acting.

TRIGGERED SEISMICITY

Triggered seismicity has been the focus of many recent studies. The 1992 Landers M7.5 earthquake showed unequivocally that large earthquakes trigger seismicity at volcanic areas as much as 1200 km distant (Hill et al. 1993). It is noteworthy that none of these areas have had eruptions for hundreds of years or more. Since 1992, many other incidences of triggered activity have been reported, mostly as small increases, such as Katmai's response to the M7.0 Karluk Lake earthquake (Power et al. 2001) and several areas in California in response to the M7.0 Hector Mine earthquake (Gomberg et al. 2001). In most cases, the onset of triggered events coincides with the arrival of the S waves, showing that dynamic effects from passing waves are involved in the response and not static effects, which are quite small especially at greater distances. Dynamic effects are approximately one order of magnitude larger than static effects (Gomberg et al. 2001). The November 3, 2002, Denali Fault earthquake (DFE) caused spectacular triggering. Hundreds of events occurred at Yellowstone (Husen et al. 2004) more than 3000 km away, and at six other areas in the western United States. A test was conducted to determine whether any of Alaska's 24 monitored active volcanoes were affected by the DFE (Sanchez & McNutt 2004). A small increase was noted at Katmai, a place with prior known triggering (Power et al. 2001); however, two other volcanoes showed decreases in seismicity. Veniaminof (1400 km SW) activity was reduced by 50% for two weeks, and Wrangell (250 km SE) was reduced by 70% for five months (Sanchez & McNutt 2004). These are apparently the first documented instances of triggered decreases in seismicity at volcanoes. Whether the fact that the Alaskan volcanoes are recently active, whereas the western U.S. cases are mostly inactive geothermal areas, may provide further clues about mechanisms.

Although most studies of triggering have involved short-term response, long-term coupling has also shown significant interaction. Marzocchi et al. (2004) demonstrated a statistically significant correlation between large earthquakes and following VEI $\geq$ 4 eruptions. The distances are up to 900 km and do not involve spatio-temporal clustering. Suggested mechanisms are related to co- and postseismic stress diffusion. An interesting study of tidal correlations for seafloor microearthquakes was performed using OBS data from Axial volcano on the Juan de Fuca Ridge (Tolstoy et al. 2002).

The considerable variety in the observations suggests that more than one mechanism is acting. Coulomb failure criteria are the most commonly modeled effects. However, a very interesting suite of observations at Grants Pass Well in Oregon, caused by interaction of waves from the Oaxaca earthquake, has provided important clues about processes in fluid saturated areas (Brodsky et al. 2003). Here the amplification factor of the well changed abruptly during the passage of waves from the earthquake and remained altered for some time. This suggests that aluminosilicate precipitate was dislodged from the fractured area adjacent to the well, increasing permeability and allowing different flow characteristics. The modeled

fracture had dimensions of order 1 mm width and 30 m length, in good agreement with observed fractures in the affected aquifer. Some other suggested mechanisms, such as rectified diffusion (Brodsky et al. 1998), may be ruled out based on quantitative modeling because the effects have too-small magnitudes (Ichihara et al. 2003).

SEISMICITY AND DEFORMATION

Major advances in recent years are the uses of the Global Positioning System (GPS) and InSAR in volcanic areas. The GPS has provided continuous and campaign data that are best suited to measure horizontal motions between pairs of stations. For InSAR, patterns of line-of-sight near vertical deformation have been measured intermittently but with unprecedented high spatial resolution in many areas that were previously inaccessible. The links with volcano seismology are indirect. Geodesy is a natural complement to seismology, so many studies seek to understand the relationship between deformation and seismicity. A spectacular recent example is the dike emplacement episode at Miyake-jima in 2000 (Toda et al. 2002), which had huge deformation signals as well as abundant seismicity.

Most InSAR studies at volcanoes have focused on positive results, that is, places are studied and reported only if anomalies are present. Typical studies show fringe patterns representing inflation or deflation, then model the deformation using Mogi sources (e.g., Pritchard & Simons 2002) or an ensemble of sources (e.g., Lu et al. 2000, Akutan Volcano). This has produced a certain amount of bias in the literature. An underutilized value of InSAR is to place constraints on volcanoes where deformation is not observed. For example, Pavlof Volcano showed no coherent deformation over the interval 1997–2001 (Mann 2002, p. 110–11). The long-term magma formation rate for Pavlof is 3.5×10^6 m^3 per year (McNutt 1999), comparable to the rate for nearby Okmok, which shows consistent deformation by InSAR. The Okmok deformation source is shallow, approximately 4 km (Mann et al. 2002). The obvious inference is that the Pavlof source is deep. Modeling shows that a source at a depth of 30 km would not produce measurable deformation at the surface (D. Mann, written communication).

A common but surprising result is the apparent inverse correlation between inflation and seismicity. A number of volcanoes with spectacular deformation are nearly aseismic. Although in some cases the seismic detection threshold is poor, existing networks were adequate to detect any significant earthquakes. Volcanoes with strong deformation but low seismicity include Westdahl (Lu et al. 2000), Peulik (Lu et al. 2002), Okmok (Lu et al. 2000), and Three Sisters (Wicks et al. 2002). Pritchard & Simons (2004) list several additional cases in South America and Kamchatka. Although models for some seismic events may be linked to magma flow (see Low-Frequency Events and Very-Long-Period Events sections, above), these InSAR observations indicate that there is significant aseismic magma movement, at least at present levels of seismic detection.

TOMOGRAPHY

Tomography remains a powerful method for determining the velocity structure beneath volcanoes. Most studies use travel times of P waves (most plentiful) or S waves (less plentiful), and a few have examined Vp/Vs (e.g., Julian et al. 1998). The velocity structures are then interpreted in terms of volcanic structures or processes, especially when other information is available, such as gravity, deformation, heat flow, etc. All such studies share the feature that the waves pass through the object of study. This is in contrast to studies of *b*-value anomalies cited above for which the anomalies occur in situ and only where the earthquakes themselves occur. Both types of studies, however, benefit from a well-distributed set of earthquakes and are complementary to each other.

Over the years the average grid size of tomography studies has gradually gotten smaller. Table 4 shows a summary of tomography studies at Kilauea on Hawaii, which has been a popular target because of its volcanic and seismic activity and its pleasant climate and surroundings. The first study in 1977 had a grid size of approximately 10 km. By 1993, this was down to 1 km. The most recent study, by Pearson (2000), used a grid size of 0.25 km. This was made possible because of data from a very dense network (McNutt et al. 1997) and a fortuitous good distribution of earthquakes. Although most studies have used damped least squares inversions, which smear out anomalies (Humphreys & Clayton 1988), the Pearson study used a composite distribution inversion (CDI), which is better at finding a smaller number of anomalous elements in a population of mostly normal ones (Clippard et al. 1995). A most interesting result of the Pearson study is the identification of a small (4 element; 0.5 by 0.5 km) Vp/Vs anomaly at the northeast edge of Halemaumau crater at a depth of 0.75 km (Figure 10*A*, see color insert), in the same location and depth as an LP event discussed by Ohminato et al. (1998), near LP events and tremor discussed by Sacorotti et al. (2001), and near VLP events studied by Alemendros et al. (2002). The Vp/Vs high is in a region of Vp low (Figure 10*B*), suggesting that the Vs must be quite low; this can be caused by the presence of gas, partial melt, or high fracture density. This encouraging result links a distinct seismic event with a very small piece of the crust shown independently to have quite different properties than the surroundings. Because of the location near the active feeder system and the high surface gas release at the northeast edge of Halemaumau, partial melt and high gas content are the preferred explanations for the Vp/Vs anomaly. Sharp Vp/Vs low anomalies have been observed at Mammoth Mountain and occurred adjacent to areas of high surface CO_2 release (Julian et al. 1998).

A number of new studies have been performed recently at small and large scales, on land and on the seafloor. Among these are a detailed study of magma storage beneath Axial Volcano, revealing a shallow low-velocity zone in the crust whose volume is between 5 and 21 km^3 (West et al. 2001). At Rabaul Volcano, Finlayson et al. (2003) imaged low-velocity zones beneath the caldera, as well as high-velocity units around the caldera rim that are interpreted to be mafic intrusive

TABLE 4 Tomography studies at Kilauea

Study	Technique	Coverage	Grid size/Node spacing	Study volume
Ellsworth & Koyanagi (1977)	Damped least-squares (Aki et al. 1977)	164 teleseismic events, recorded at 26 stations. 2112 P-wave arrivals	x–y: 7.5 km, z: 12.5 km (first layer), 15 km	x–y: 67.5 × 67.5 km, z: 72.5 km
Thurber (1984)	Parameter separation and approximate ray tracing (ART)/damped least-squares	85 local earthquakes, recorded at 17 stations	x: 4 km, y–z: 3 km	x: 30 km y: 20 km z: 10 km
Rowan & Clayton (1993)	Iterative back projection/damped least-squares	12,295 local earthquakes, recorded at 42 stations. 111,600 P-wave arrivals	Two grid sizes: 1 × 1 × 1 km and 5 × 5 × 5 km	2 regions: x: 100, 60 km, y: 55, 30 km, z: 50, 50 km
Okubo et al. (1997)	Finite difference ray tracing (Benz et al. 1996)/damped least-squares	4754 local earthquakes, recorded at 42 stations	x–y: 1 km, z: 2 km	x: ~95 km, y: ~55 km, z: 11 km
Dawson et al. (1999)	Finite difference ray tracing (Benz et al. 1996)/damped least-squares. Vp/Vs structure also determined*	206 local earthquakes, recorded at 67 stations. 4695 P- and 3195 S-wave arrivals	0.5 × 0.5 × 0.5 km	Vp: 15 × 15 × 15 km Vp/Vs: x–y: 10 × 10 km z: 5 km
Pearson (2000)	Composite distribution inversion (CDI) Vp and Vp/Vs	271 earthquakes recorded at more than 100 stations	0.25 × 0.25 × 0.25 km	x–y: 10 × 10 km z: 6 km

rocks. Foulger et al. (2001) determined Vp, Vs, and Vp/Vs for the upper mantle beneath Iceland. They found a 200–250-km-wide low-velocity zone with Vp lower by up to 2.7% and Vs by 4.9%, consistent with approximately 2% partial melt. The anomaly extends to a depth of approximately 450 km and is more or less cylindrical in the upper part but more tabular at depth, suggesting basal heating and a shallow origin for the Iceland hotspot rather than a deep mantle plume.

Several persistent problems occur with tomography studies. One problem is the lack of error resolution. This is generally done synthetically by generating a checkerboard pattern of high- and low-velocity anomalies. The real rays are then used to determine how well the checkerboard can be recovered from the data using the same methods as for the real data. The recovered checkerboard can then be used to compare areas of good and bad resolution in the actual data. A second problem is the lack of convergence of iterations of the analyses. Generally, the model velocities are adjusted at each iteration step, then travel times are recalculated for the events, then model velocities adjusted again based on the new travel times, and so on. The variance reduction at each step is computed, and the procedure is stopped when the variance reduction becomes negligible. However, this procedure does not guarantee that an absolute variance reduction, or optimal model, has been reached. The final model may be a local minimum and to a certain extent arbitrary. In everyday language: Read the fine print!

CONCLUDING REMARKS

Although this paper does not require a conclusion that ties all the elements together, it may be instructive to discuss briefly two issues: How the topics were chosen and likely future trends and needs.

The topics were chosen to be timely; a visit to nearly any recent conference on volcanic seismology would include the topics presented here. The topics are also relevant to many of the scientific problems of volcanology that can be addressed via seismology. I added some new material where appropriate; although, in most cases the examples are drawn from current literature. Most of the topics, while in the domain of seismology per se, involve some elements from related fields. Indeed, the integration of various data sets has greatly improved the ability to place constraints on models. I sought a balance between topics that are simple but important, such as the identification of two possible processes in swarms (e.g., Figure 4), and topics that require sophisticated methods and large data sets (e.g., tomography). I attempted to address important areas in a substantial way. Finally, I chose topics with which I am familiar.

The future offers the likelihood of better data, that is, a higher number of stations and higher numbers of broadband, high-dynamic-range, three-component stations. We are nearing the stage of uniform seismic coverage of entire arcs. The Plate Boundary Observatory (PBO) and USArray components of Earthscope (http://www.earthscope.org) will dramatically increase instrumental coverage of the western United States and will be a huge benefit to the scientific community.

In Japan, the GEONET (GPS) and NEID Hi-net (seismic) networks are already paying huge dividends. To date, we have not yet caught a large (VEI > 4) eruption with local, on-scale, modern instruments; when it happens, I am sure it will be a scientific bonanza. Careful readers may have noted the large proliferation of models for LF/LP events. It appears that either the existing data are not sufficient to rule out models or that there is enough nonuniqueness to permit many models. Perhaps the field would benefit from a controlled experiment in which all participants would have access to the same data, and models could then be compared with a (known) source to allow true testing of the models. Finally, the emergence of GPS and InSAR, roughly 12 years ago, has had profound effects on volcanic seismology. It is probable that completely new technology will emerge and provide tremendous new insights. Volcanic seismology is likely to remain a very active and dynamic branch of Earth science.

ACKNOWLEDGMENTS

I thank John Sanchez and Celso Reyes for reviews and help with the figures, and Jennifer Risse for help with the tables. I am grateful to my AVO colleagues for their support, and to the many friends and colleagues who have sent reprints and shared ideas and discoveries over the years.

The *Annual Review of Earth and Planetary Science* is online at http://earth.annualreviews.org

LITERATURE CITED

Aki K, Christoffersson C, Husebye ES. 1977. Determination of the three-dimensional seismic structure of the lithosphere. *J. Geophys. Res.* 82:277–96

Aki K, Koyanagi RY. 1981. Deep volcanic tremor and magma ascent mechanism under Kilauea, Hawaii. *J. Geophys. Res.* 86:7095–110

Alemandros J, Chouet B, Dawson P, Bond T. 2002. Identifying elements of the plumbing system beneath Kilauea Volcano, Hawaii, from the source locations of very-long-period signals. *Geophys. J. Int.* 148:303–12

Archuleta RJ, Cranswick E, Mueller C, Spudich P. 1982. Source parameters of the 1980 Mammoth Lakes, California, earthquake sequence. *J. Geophys. Res.* 87:4595–607

Aster R, McIntosh W, Kyle P, Esser R, Bartel B, et al. 2004. Real-time data received from Mount Erebus volcano, Antarctica. *EOS Trans. Am. Geophys. Union* 85:97100–1

Bath M. 1981. Earthquake magnitude—recent research and current trends. *Earth. Sci. Rev.* 17:315–98

Battaglia J, Got J-L, Okubo P. 2003. Location of long-period events below Kilauea Volcano using seismic amplitudes and accurate relative relocation. *J. Geophys. Res.* 108:10.1029/2002JB002517

Battaglia J, Thurber CL, Got J-L, Rowe CA, White RA. 2004. Precise relocation of earthquakes following the June 15, 1991 explosion of Mount Pinatubo (Philippines). *J. Geophys. Res.* 109:In press

Benoit JP, McNutt SR. 1997. New constraints on source processes of volcanic tremor at Arenal Volcano, Costa Rica, using broadband seismic data. *Geophys. Res. Lett.* 24: 449–52

Benoit JP, McNutt SR, Barboza V. 2003. The duration-amplitude distribution of volcanic tremor. *J. Geophys. Res.* 108:10.1029/2001JB001520

Benz HM, Chouet BA, Dawson PB, Lahr JC, Page RA, Hole JA. 1996. Three-dimensional P and S wave velocity structure of Redoubt Volcano, Alaska. *J. Geophys. Res.* 101:8111–28

Brodsky EE, Roeloffs E, Woodcock D, Gall I, Manga M. 2003. A mechanism for sustained groundwater pressure changes induced by distant earthquakes. *J. Geophys. Res*. 108:10.1029/2002JB002321

Brodsky EE, Sturtevant B, Kanamori H. 1998. Earthquakes, volcanoes, and rectified diffusion. *J. Geophys. Res.* 103:23827–38

Caplan-Auerbach J, McNutt SR. 2003. New insights into the 1999 eruptions of Shishaldin Volcano based on acoustic data. *Bull. Volcanol*. 65:405–17

Centamore C, Patane G, Tuve T. 1999. Maximum entropy estimation of *b*-values at Mt Etna: comparison with conventional least squares and maximum likelihood results and correlation with volcanic activity. *Ann. Geofis.* 42:515–28

Chiarabba C, Amato A, Boschi E, Barberi F. 2000. Recent seismicity and tomographic modeling of the Mount Etna plumbing system. *J. Geophys. Res.* 105:10923–38

Chouet BA. 1996. Long-period volcano seismicity: its source and use in eruption forecasting. *Nature* 380:309–16

Clippard JD, Christensen DH, Rechtien RD. 1995. Composite distribution inversion applied to crosshole tomography. *Geophysics* 60:1283–94

Dawson PB, Chouet BA, Okubo P, Villasenor A, Benz HM. 1999. Three-dimensional velocity structure of the Kilauea caldera, Hawaii. *Geophys. Res. Lett.* 26:2805–8

Dragert H, Wang KL, James TS. 2001. A silent slip event on the deeper Cascadia subduction interface. *Science* 292:1525–28

Ellsworth WL, Koyanagi RY. 1977. Three-dimensional crust and mantle structure of Kilauea Volcano, Hawaii. *J. Geophys. Res.* 82:5379–94

Falsaperla S, Graziani S, Nunnari G, Spampinato S. 1996. Automatic classification of volcanic earthquakes by using multi-layered neural networks. *Nat. Hazards* 13:205–28

Finlayson DM, Gudmundsson O, Itikarai I, Nishimura Y, Shimamura H. 2003. Rabaul volcano, Papua New Guinea: seismic tomographic imaging of an active caldera. *J. Volcanol. Geotherm. Res.* 124:153–71

Foulger GR, Pritchard MJ, Julian BR, Evand JR, Allen RM, et al. 2001. Seismic tomography shows that upwelling beneath Iceland is confined to the upper mantle. *Geophys. J. Int.* 146:504–30

Frolich C, Davis S. 1993. Teleseismic *b*-values: or much ado about 1.0. *J. Geophys. Res.* 98:631–34

Fujita E, Ida Y. 2003. Geometrical effects and low-attenuation resonance of volcanic fluid inclusions for the source mechanism of long-period earthquakes. *J. Geophys. Res.* 108:10.1029/2002JB001806

Garces MA. 2000. Theory of acoustic propagation in a multi-phase stratified liquid flowing within an elastic-walled conduit of varying cross-sectional area. *J. Volcanol. Geotherm. Res.* 101:1–17

Garces MA, Hagerty MT, Schwartz SY. 1998. Magma acoustics and time-varying melt properties at Arenal Volcano, Costa Rica. *Geophys. Res. Lett.* 25:2293–96

Gomberg J, Reasenberg PA, Bodin P, Harris RA. 2001. Earthquake triggering by seismic waves following the Landers and Hector Mine earthquakes. *Nature* 411:462–66

Gresta S, Patane G. 1983. Variation of b values before the Etnean eruption of March-August 1983. *Pure Appl. Geophys.* 121:903–12

Haar LC, Mueller CS, Fletcher JB, Boore DM. 1986. Comments on "Some recent Lg phase displacement spectral densities and their implications with respect to prediction of ground motions in Eastern North America" by R. Street. *Bull. Seis. Soc. Am.* 76:291–95

Hellweg M. 2000. Physical models for the source of Lascar's harmonic tremor. *J. Volcanol. Geotherm. Res*. 101:183–98

Hill DP. 1996. Earthquakes and carbon dioxide beneath Mammoth Mountain, California. *Seis. Res. Lett.* 67:8–15

Hill DP, Pollitz F, Newhall C. 2002. Earthquake-volcano interactions. *Phys. Today* 55: 41–47

Hill DP, Reasenberg PA, Michael A, Arabaz WJ, Beroza G, et al. 1993. Seismicity remotely triggered by the magnitude 7.3 Landers, California earthquake. *Science* 260: 1617–23

Humphreys E, Clayton RW. 1988. Adaptation of back projection tomography to seismic travel time problems. *J. Geophys. Res.* 93:1073–85

Husen S, Taylor R, Smith RB, Healser H. 2004. Changes in geyser eruption behavior and remotely triggered seismicity in Yellowstone National Park produced by the 2002 M 7.9 Denali fault earthquake, Alaska. *Geology* 32:537–40

Ichihara M, Brodsky EE, Kanamori H. 2003. Reconsideration of the effect of rectified diffusion in volcanic-seismic systems. *Gen. Assem. Int. Union Geodesy Geophys., Sapporo, Jpn.*, Abstr. Vol., JSV04/01P/D-001

Iguchi M. 1995. A vertical expansion source model for the mechanisms of earthquakes originated in the magma conduit of an andesitic volcano: Sakurajima, Japan. *Bull. Volcanol. Soc. Jpn.* 39:49–67

Jimenez Z, Reyes G, Espindola JM. 1995. The July 1994 episode of seismic activity at Colima Volcano, Mexico. *J. Volcanol. Geotherm. Res.* 64:321–26

Johnson JB. 2000. *Interpretation of infrasound generated by erupting volcanoes and seismoacoustic energy partitioning during Strombolian explosions*. PhD thesis. Univ. Wash., Seattle. 159 pp.

Jolly AD, McNutt SR. 1999. Relationship between *b*-values and maximum depths of seismicity at Martin and Mageik volcanoes, Katmai National Park, Alaska; July 1995-December 1997. *J. Volcanol. Geotherm. Res.* 93:173–90

Julian BR. 1994. Volcanic tremor: nonlinear excitation by fluid flow. *J. Geophys. Res*. 99: 11859–77

Julian BR, Miller AD, Foulger GR. 1997. Non-double-couple earthquake mechanisms at the Hengill-Grensdalur volcanic complex, southwest Iceland. *Geophys. Res. Lett.* 24:743–46

Julian BR, Pitt AM, Foulger GR. 1998. Seismic image of a CO_2 reservoir beneath a seismically active volcano. *Geophys. J. Int.* 133:F7–10

Kanamori H, Given JW. 1992. Analysis of long period seismic waves excited by the May 18, eruption of Mount St. Helens: a terrestrial monopole? *J. Geophys. Res.* 87:5422–32

Kanamori H, Mori J. 1992. Harmonic excitation of mantle Rayleigh waves by the 1991 eruption of Mount Pinatubo, Philippines. *Geophys. Res. Lett.* 19:721–24

Kaneshima S, Kawakatsu H, Matsubayashi H, Sudo Y, Tsutsui T, et al. 1996. Mechanism of phreatic eruptions at Aso Volcano inferred from near-field broadband seismic observations. *Science* 273:642–45

Kawakatsu H, Kaneshima S, Matsubayashi H, Ohminato T, Sudo Y, et al. 2000. Aso94: Aso seismic observation with broadband instruments. *J. Volcanol. Geotherm. Res.* 101:129–54

Kawakatsu H, Ohminato T, Ito H. 1994. 10s-Period volcanic tremors observed over a wide area in southwestern Japan. *Geophys. Res. Lett.* 21:1963–66

Kawakatsu H, Ohminato T, Ito H, Kuwahara Y, Kato T, et al. 1992. Broadband seismic observation at the Sakurajima Volcano, Japan. *Geophys. Res. Lett.* 19:1959–62

Kilburn CRJ. 2003. Multiscale fracturing as a key to forecasting volcanic eruptions. *J. Volcanol. Geotherm. Res.* 125:271–89

Kumagai H, Miyakawa K, Negishi H, Inoue H, Obara K, Suetsugu D. 2003. Magmatic dike resonances inferred from very-long-period seismic signals. *Science* 299:2058–61

Kumagai H, Ohminato T, Nakano M, Ooi M, Kubo A, et al. 2001. Very-long-period seismic signals and caldera formation at Miyake Island, Japan. *Science* 293:687–90

Lahr J, Page RA, Chouet BA, Stephens CD, Harlow DH, et al. 1994. Seismic evolution of the 1989–90 eruption sequence of Redoubt Volcano, Alaska. *J. Volcanol. Geotherm. Res.* 62:69–94

Lees JM, Wu H. 1999. P wave anisotropy, stress, and crack distribution at Coso geothermal field, California. *J. Geophys. Res.* 104: 17955–73

Lu Z, Mann D, Freymueller JT, Meyer DJ. 2000. Synthetic aperture radar interferometry of Okmok volcano, Alaska: Radar observations. *J. Geophys. Res.* 105:10791–806

Lu Z, Wicks JC, Dzurisin D, Power JA, Moran SC, Thatcher W. 2002. Magmatic inflation at a dormant stratovolcano: 1996–1998 activity at Mount Peulik volcano, Alaska, revealed by satellite radar interferometry. *J. Geophys. Res.* 107:10.1029/2001JB000471

Lu Z, Wicks JC, Dzurisin D, Thatcher W, Freymueller JT, et al. 2000. Aseismic inflation of Westdahl Volcano, Alaska, revealed by satellite radar interferometry. *Geophys. Res. Lett.* 27:1567–70

Lu Z, Wicks JC, Power JA, Dzurisin D. 2000. Deformation of Akutan volcano, Alaska, revealed by satellite radar interferometry. *J. Geophys. Res.* 105:21483–496

Main IG. 1981. A characteristic earthquake model of the seismicity preceding the eruption of Mount St Helens on 18 May 1980. *Phys. Earth Planet. Int*. 49:283–93

Malone SD, Endo ET, Weaver CS, Ramey JW. 1981. Seismic monitoring for eruption prediction. *U.S. Geol. Survey Prof. Pap. 1250*, pp. 803–13

Mann D. 2002. *Deformation of Alaskan volcanoes measured using SAR interferometry and GPS*. PhD thesis. Univ. Alaska, Fairbanks. 122 pp.

Mann D, Freymueller J, Lu Z. 2002. Deformation associated with the 1997 eruption of Okmok volcano, Alaska. *J. Geophys. Res.* 107:10.1029/2001JB000163

Marzocchi W, Zaccarelli L, Boschi E. 2004. Phenomenological evidence in favor of remote seismic coupling for large volcanic eruptions. *Geophys. Res. Lett.* 31:10.1029/2003GL018709

McNutt SR. 1989. Analysis of earthquake spectra from Long Valley, California, using the NEWT seismic system. *Calif. Div. Mines Geol. Open-File Rep. 89–6*. 46 pp.

McNutt SR. 1994a. Volcanic tremor amplitude correlated with volcano explosivity and its potential use in determining ash hazards to aviation. *U.S. Geol. Survey Bull. 2047*, pp. 377–85

McNutt SR. 1994b. Volcanic tremor from around the world: 1992 update. *Acta Vulcanol.* 5:197–200

McNutt SR. 1996. Seismic monitoring and eruption forecasting of volcanoes: A review of the state-of-the-art and case histories. In *Monitoring and Mitigation of Volcano Hazards*, ed. R Scarpa, R Tilling, pp. 99–146. Berlin/Heidelberg: Springer-Verlag. 841 pp.

McNutt SR. 1999. Eruptions of Pavlof Volcano, Alaska, and their possible modulation by Ocean load and Tectonic stresses: Re-evaluation of the hypothesis based on New Data from 1984–1998. *Pure Appl. Geophys.* 155:701–12

McNutt SR, Ida Y, Chouet BA, Okubo P, Oikawa J, Saccorotti G. 1997. Kilauea Volcano provides Hot Seismic Data for Joint Japanese-US Experiment. *EOS Trans. Am. Geophys. Union* 78:105–111

Minakami T. 1974. Seismology of volcanoes in Japan. In *Developments in Solid Earth Geophysics. Physical Volcanology*, ed. L Civetta, P Gasparini, G Luongo, A Rapolla, 6:1–27. Amsterdam: Elsevier

Mora MM, LeSage P, Dorel J, Bard P-Y, Metaxian J-P, et al. 2001. Study of seismic site effects using H/V spectral ratios at Arenal Volcano, Costa Rica. *Geophys. Res. Lett.* 28:2991–94

Moran SC. 2003. Multiple seismogenic processes for high-frequency earthquakes at Katmai National Park, Alaska: Evidence

from stress tensor inversions of fault-plane solutions. *Bull. Seis. Soc. Am.* 93:94–108

Murru M, Montuori C, Wyss M, Privitera E. 1999. The locations of magma chambers at Mt. Etna, Italy, mapped by *b*-values. *Geophys. Res. Lett.* 26:2553–56

Nakano M, Kumagai H, Kumazawa M, Yamaoka K, Chouet BA. 1998. The excitation and characteristic frequency of the long-period volcanic event: An approach based on an inhomogeneous autoregressive model of a linear dynamic system. *J. Geophys. Res.* 103:10,031–046

Neuberg J. 2000. Characteristics and causes of shallow seismicity in andesite volcanoes. *Philos. Trans. R. Soc. London Ser. A* 358:1533–46

Neuberg J, Luckett R, Baptie B, Olsen K. 2000. Models of tremor and low-frequency earthquake swarms on Montserrat. *J. Volcanol. Geotherm. Res.* 101:83–104

Neuberg J, Luckett R, Ripepe M, Braun T. 1994. Highlights from a seismic broadband array on Stromboli volcano. *Geophys. Res. Lett.* 21:749–52

Neuberg J, O'Gorman C. 2002. A model of the seismic wavefield in gas-charged magma: application to Soufriere Hills Volcano, Montserrat. In *The Eruption of Soufriere Hills Volcano, Montserrat, from 1995 to 1999*, ed. TH Druitt, BP Kokelaar, Geol. Soc. London, Memo. 21:603–9

Nishimura T, Chouet B. 2003. A numerical simulation of magma motion, crustal deformation, and seismic radiation associated with volcanic eruptions. *Geophys. J. Int.* 153:699–718

Nishimura T, Nakamichi H, Tanaka S, Sato M, Kobayashi T, et al. 2000. Source process of very long period seismic events associated with the 1998 activity of Iwate Volcano, northeastern Japan. *J. Geophys. Res.* 105:19135–47

Obara K. 2002. Nonvolcanic deep tremor associated with subduction in southwest Japan. *Science* 296:1679–81

Ohminato T, Chouet BA, Dawson P, Kedar S. 1998. Waveform inversion of very long period impulsive signals associated with magmatic injection beneath Kilauea Volcano, Hawaii. *J. Geophys. Res.* 103:23839–62

Ohminato T, Ereditato D. 1997. Broadband seismic observations at Satsuma-Iwojima volcano, Japan. *Geophys. Res. Lett.* 24: 2845–48

Okubo PG, Benz HM, Chouet BA. 1997. Imaging the crustal sources beneath Mauna Loa and Kilauea volcanoes, Hawaii. *Geology* 25:867–70

Pearson AD. 2000. *The three-dimensional structure of the summit magma complex at Kilauea Volcano, Hawaii, from travel time CDI tomography*. MS thesis. Univ. Alaska Fairbanks. 97 pp.

Power JA, Jolly AD, Page RA, McNutt SR.1995. Seismicity and forecasting of the 1992 eruptions of Crater Peak vent, Mount Spurr Volcano, Alaska: An overview. In *The 1992 Eruptions of Crater Peak Vent, Mount Spurr Volcano, Alaska*, ed. TEC Keith, pp. 149–59. U.S. Geol. Survey Bull. 2139

Power JA, Moran SC, McNutt SR, Stihler SD, Sanchez JJ. 2001. Seismic response of the Katmai volcanoes to the 6 December 1999 magnitude 7.0 Karluk Lake earthquake, Alaska. *Bull. Seis. Soc. Am.* 91:57–63

Power JA, Stihler SD, White RA, Moran SC. 2004. Observations of deep long-period (DLP) seismic events beneath Aleutian arc volcanoes; 1989–2002. *J. Volcanol. Geotherm. Res.* 138:243–66

Power JA, Wyss M, Latchman JL. 1998. Spatial variations in the frequency-magnitude distribution of earthquakes at Soufriere Hills volcano, Montserrat, West Indies. *Geophys. Res. Lett.* 25:3653–56

Prejean S, Ellsworth WE, Zoback M, Waldhauser F. 2002. Fault structure and kinematics of the Long Valley caldera region, California, revealed by high-accuracy earthquake hypocenters and focal mechanism stress inversions. *J. Geophys. Res.* 107:10.1029/2001JB001168

Pritchard ME, Simons M. 2002. A satellite geodetic survey of large-scale deformation

of volcanic centres in the central Andes. *Nature* 418:167–71

Pritchard ME, Simons M. 2004. Surveying volcanic arcs with radar interferometry: The central Andes, Kamchatka, and beyond. *Geology* 14(8):4–11

Richter C. 1958. *Elementary Seismology*. San Francisco: Freeman. 768 pp.

Rowan LR, Clayton RW. 1993. The three-dimensional structure of Kilauea Volcano, Hawaii, from travel time tomography. *J. Geophys. Res.* 98:4355–75

Rowe CA, Aster RC, Borchers B, Young CJ. 2002. An automatic, adaptive algorithm for refining phase picks in large seismic data sets. *Bull. Seis. Soc. Am.* 92:1660–74

Rowe CA, Aster RC, Kyle PR, Dibble RR, Schlue JW. 2000. Seismic and acoustic observations at Mount Erebus volcano, Ross Island, Antarctica, 1994–1998. *J. Volcanol. Geotherm. Res.* 101:105–28

Rowe CA, Aster RC, Kyle PR, Schlue JW, Dibble RR. 1998. Broadband recording of strombolian explosions and associated very-long period seismic signals on Mount Erebus volcano, Ross Island, Antarctica. *Geophys. Res. Lett.* 25:297–300

Saccorotti G, Chouet B, Dawson P. 2001. Wavefield properties of a shallow long-period event and tremor at Kilauea Volcano, Hawaii. *J. Volcanol. Geotherm. Res.* 108:163–89

Sanchez JJ, McNutt SR. 2004. Intermediate-term declines in seismicity at Mt. Wrangell and Mt. Veniaminof volcanoes, Alaska, following the November 3, 2002, Mw 7.9 Denali fault earthquake. *Bull. Seis. Soc. Am.* 94(6):In press

Sanchez JJ, McNutt SR, Power JA, Wyss M. 2004. Spatial variations in the frequency-magnitude distribution of earthquakes at Mount Pinatubo volcano. *Bull. Seis. Soc. Am.* 94:430–38

Sanchez JJ, Wyss M, McNutt SR. 2004. Temporal-spatial variations of stress at Redoubt Volcano, Alaska, inferred from inversion of fault plane solutions. *J. Volcanol. Geotherm. Res.* 130:1–30

Sohn RA, Hildbrand JA, Webb SC. 1999. A microearthquake survey of the high-temperature vent fields on the volcanically active East Pacific Rise (9°50′N). *J. Geophys. Res.* 104:25367–77

Suzuki S, Kasahara M. 1979. Seismic activity immediately before and in the early stage of the 1977 eruption of Usu Volcano, Hokkaido, Japan. *J. Fac. Sci., Hokkaido Univ. Ser. VII*, 6:239–54

Thurber CH. 1984. Seismic detection of the summit magma complex of Kilauea Volcano, Hawaii. *Science* 223:165–67

Toda S, Stein RS, Sagiya T. 2002. Evidence from AD 2000 Izu islands earthquake swarm that stressing rate governs seismicity. *Nature* 419:58–61

Tolstoy M, Vernon FL, Orcutt JA, Wyatt FK. 2002. Breathing of the seafloor: Tidal correlations of seismicity at Axial volcano. *Geology* 30:503–6

Uhira K, Takeo M. 1994. The source of explosive eruptions of Sakurajima Volcano, Japan. *J. Geophys. Res.* 99:17775–789

Uhira K, Yamasoto H, Takeo M. 1994. Source mechanism of seismic waves exited by pyroclastic flows observed at Unzen volcano. *J. Geophys. Res.* 99:17757–773

Ukawa M. 1993. Excitation mechanism of large amplitude volcanic tremor associated with the 1989 Ito-oki submarine eruption, central Japan. *J. Volcanol. Geotherm. Res.* 55:33–50

Waite GP, Smith RB. 2004. Seismotectonics and stress field of the Yellowstone volcanic plateau from earthquake first-motions and other indicators. *J. Geophys. Res.* 109:10.1029/2003JB002675

Waldhauser F, Ellsworth WL. 2000. A double-difference earthquake location algorithm: Method and application to the northern Hayward fault, California. *Bull. Seis. Soc. Am.* 90:1353–68

Warren NW, Latham GV. 1970. An experimental study of thermally induced microfracturing and its relation to volcanic seismicity. *J. Geophys. Res.* 75:4455–64

West M, Menke W, Tolstoy M, Webb S, Sohn R. 2001. Magma storage beneath Axial

volcano on the Juan de Fuca mid-ocean ridge. *Nature* 413:833–36

White RA. 1996. Precursory seismicity and forecasting of the June 15, 1991 eruption of Mount Pinatubo, Philippines. In *Fire and Mud: Eruptions and Lahars of Mount Pinatubo, Philippines*, ed. CG Newhall, RS Punongbayan, pp. 285–305. Seattle: Univ. Wash. Press. 1126 pp.

Wicks CW, Dzurisin D, Ingebritsen S, Thatcher W, Lu Z, Iverson J. 2002. Magmatic activity beneath the quiescent Three Sisters volcanic center, central Oregon Cascade Range, USA. *Geophys. Res. Lett.* 29: 10.1029/2001GL014205

Wiemer S, Benoit JP. 1996. Mapping the *b*-value anomaly at 100 km depth in Alaska and New Zealand subduction zones. *Geophys. Res. Lett.* 23:1557–60

Wiemer S, McNutt SR. 1997. Variations in the frequency-magnitude distribution with depth in two volcanic areas: Mount St Helens, Washington, and Mt. Spurr, Alaska. *Geophys. Res. Lett.* 24:189–92

Wiemer S, McNutt SR, Wyss M. 1998. Temporal and three-dimensional spatial analyses of the frequency-magnitude distribution near Long Valley Caldera, California. *Geophys. J. Int.* 134:409–21

Wilson EK, McNutt SR. 1998. Parameters of the generic volcanic earthquake swarm model. *EOS Trans. Am. Geophys. Union* 79: 45, F962 (Abstr.)

Wyss M. 1973. Towards a physical understanding of the earthquake frequency distribution. *Geophys. J. R. Astron. Soc*. 31:341–59

Wyss M, Klein F, Nagamine K, Wiemer S. 1998. Anomalously high *b*-values in the south flank of Kilauea Volcano, Hawaii: evidence for the distribution of magma below Kilauea's east rift zone. *J. Volcanol. Geotherm. Res.* 106:23–37

Wyss M, Shimazaki S, Wiemer S. 1997. Mapping active magma chambers beneath the off-Ito volcano, Japan. *J. Geophys. Res.* 102:413–20

Yamamoto M, Kawakatsu H, Kaneshima S, Mori T, Tsutsui T, et al. 1999. Detection of a crack-like conduit beneath the active crater at Aso volcano, Japan. *Geophys. Res. Lett.* 26:3677–80

Zhang H, Thurber CH. 2003. Double-difference tomography: The method and its application to the Hayward Fault, California. *Bull. Seis. Soc. Am.* 93:1875–89

Zobin VM, ed. 2003. Introduction to volcanic seismology. *Developments in Volcanology*, Volume 6. Amsterdam: Elsevier. 290 pp.

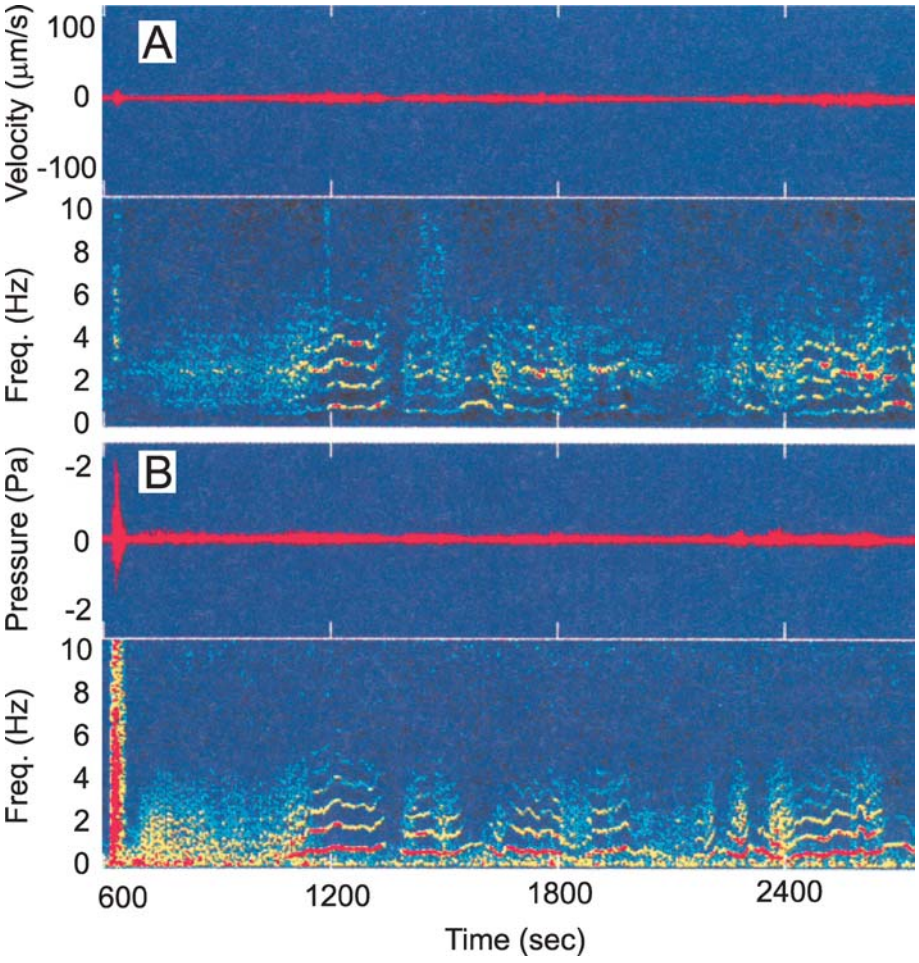

Figure 7 Forty minutes of seismic and acoustic data from Arenal Volcano, Costa Rica. (*A*) Velocity seismogram (*vertical component*) and corresponding spectrogram showing the normalized log of the power spectral density as a function of time. Blue colors represent low signal strength, yellow medium, and red strong. (*B*) The airborne acoustic pressure recorded for the same time period and its corresponding spectrogram. Note the evenly spaced spectral peaks of both the volcanic tremor and the acoustic signal; the same frequencies show for both and glide in the same way, demonstrating the coupling of the energy across the air-ground interface (modified from Garces et al. 1998).

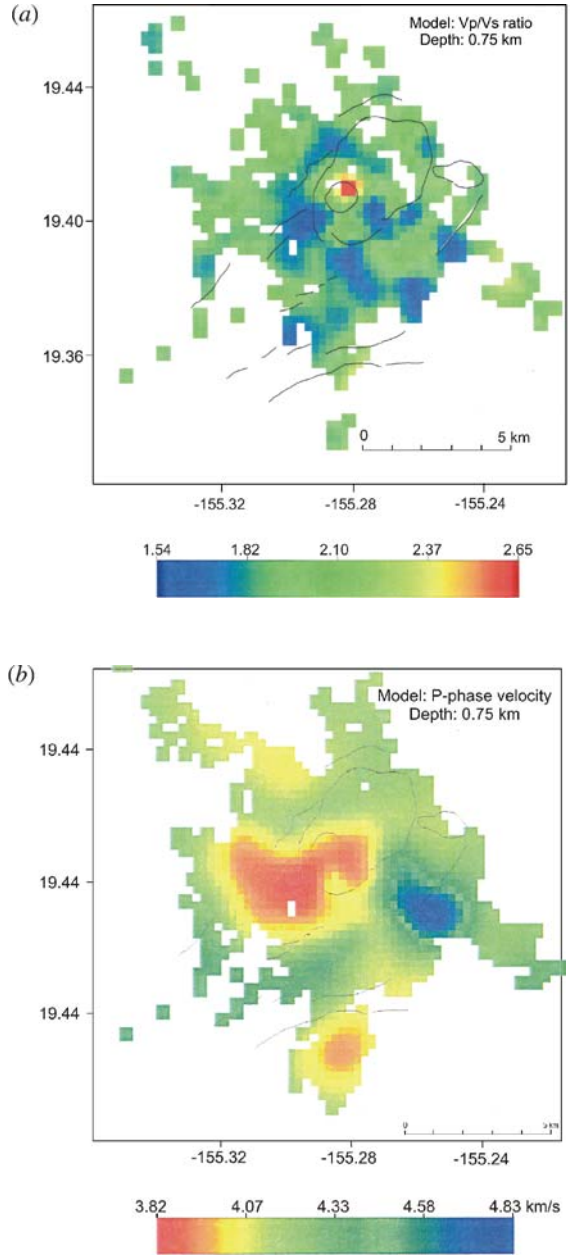

See legend on next page

Figure 10 Composite distribution inversion tomography plots for Kilauea summit region. Outlines of Kilauea caldera and Halemaumau crater and prominent faults are shown as black lines. (*A*) Vp/Vs for layer at 0.75 depth, 0.25 km thick. Blocks are 250 m in size. Red colors indicate high Vp/Vs, green normal, and blue low. Note the small high Vp/Vs anomaly near the edge of Halemaumau crater. This is the same location as a well-studied LP event (see text). (*B*) Vp for layer at 0.75 depth, 0.25 km thick. Red colors indicate low Vp, green normal, and blue high. Note the broad Vp low surrounding and southwest of Halemaumau, and the Vp high near the west end of the East Rift Zone (modified from Pearson 2000).

Annual Review of Earth and Planetary Sciences
Volume 33, 2005

CONTENTS